agronomy

MDPI

Article

Semi-Transparent Organic Photovoltaics Applied as Greenhouse Shade for Spring and Summer Tomato Production in Arid Climate

Rebekah Waller [1], Murat Kacira [1,*], Esther Magadley [2], Meir Teitel [3] and Ibrahim Yehia [2]

[1] Department of Biosystems Engineering, The University of Arizona, Tucson, AZ 85721, USA; rebekahewaller@email.arizona.edu
[2] Triangle Research and Development Center, P.O. Box 2167, Kfar-Qari 30075, Israel; esther.magadley@gmail.com (E.M.); yehia1002@gmail.com (I.Y.)
[3] Institute of Agricultural Engineering, Agricultural Research Organization, The Volcani Center, HaMaccabim Road 68, P.O. Box 15159, Rishon LeZion 7528809, Israel; grteitel@volcani.agri.gov.il
* Correspondence: mkacira@arizona.edu

Abstract: Recognizing the growing interest in the application of organic photovoltaics (OPVs) with greenhouse crop production systems, in this study we used flexible, roll-to-roll printed, semi-transparent OPV arrays as a roof shade for a greenhouse hydroponic tomato production system during a spring and summer production season in the arid southwestern U.S. The wavelength-selective OPV arrays were installed in a contiguous area on a section of the greenhouse roof, decreasing the transmittance of all solar radiation wavelengths and photosynthetically active radiation (PAR) wavelengths (400–700 nm) to the OPV-shaded area by approximately 40% and 37%, respectively. Microclimate conditions and tomato crop growth and yield parameters were measured in both the OPV-shaded ('OPV') and non-OPV-shaded ('Control') sections of the greenhouse. The OPV shade stabilized the canopy temperature during midday periods with the highest solar radiation intensities, performing the function of a conventional shading method. Although delayed fruit development and ripening in the OPV section resulted in lower total yields compared to the Control section (24.6 kg m^{-2} and 27.7 kg m^{-2}, respectively), after the fourth (of 10 total) harvests, the average weekly yield, fruit number, and fruit mass were not significantly different between the treatment (OPV-shaded) and control group. Light use efficiency (LUE), defined as the ratio of total fruit yield to accumulated PAR received by the plant canopy, was nearly twice as high as the Control section, with 21.4 g of fruit per mole of PAR for plants in the OPV-covered section compared to 10.1 g in the Control section. Overall, this study demonstrated that the use of semi-transparent OPVs as a seasonal shade element for greenhouse production in a high-light region is feasible. However, a higher transmission of PAR and greater OPV device efficiency and durability could make OPV shades more economically viable, providing a desirable solution for co-located greenhouse crop production and renewable energy generation in hot and high-light intensity regions.

Keywords: organic photovoltaics; greenhouses; tomato; shading; arid region

Citation: Waller, R.; Kacira, M.; Magadley, E.; Teitel, M.; Yehia, I. Semi-Transparent Organic Photovoltaics Applied as Greenhouse Shade for Spring and Summer Tomato Production in Arid Climate. *Agronomy* **2021**, *11*, 1152. https://doi.org/10.3390/agronomy11061152

Academic Editors: Miguel-Ángel Muñoz-García and Luis Hernández-Callejo

Received: 18 May 2021
Accepted: 31 May 2021
Published: 4 June 2021

1. Introduction

Greenhouse-integrated photovoltaic (PV) technologies are increasingly seen as a promising solution for sustainable greenhouse agriculture. Higher annual yields and lower water consumption compared to conventional farming make greenhouse production particularly attractive for space-limited and water-limited regions. However, the climate control systems and other electrical components involved in greenhouse operations consume large amounts of energy [1,2]. PV systems that are structurally integrated with the greenhouse enable the co-production of renewable energy and crops on the same land footprint, which is advantageous from a resource-use efficiency perspective [3].

Different types of PV technologies have been tested for integration with greenhouse systems. One design strategy for PV integration with greenhouses involves the positioning of conventional opaque PVs (conv-PVs) along the greenhouse structure with gaps between them, thereby allowing a fraction of sunlight to enter the greenhouse. The challenge in this is ascertaining the correct percentage of roof coverage, balancing PV electricity generation with adequate lighting conditions inside the greenhouse [4,5]. In order to provide more control of the lighting conditions in the greenhouse with integrated conv-PVs, some have proposed designs with dynamically-controlled PV blind systems that can respond to outdoor conditions and sunlight variations [6–8].

Thin-film semi-transparent or transparent PV technologies (STPV), despite showing relatively lower efficiencies compared to conv-PV, are gaining attention for their application to greenhouse structures. In contrast to conv-PV, STPV absorbs only a portion of incident light for electricity generation, leaving unabsorbed photons available for plant photosynthesis [9,10]. Recent advances in fabrication methods have enabled significant progress in thin-film STPV development [11]. There are many types of technologies within this emerging class of PV (e.g., copper indium gallium selenide, cadmium telluride, amorphous silicon, perovskite, dye-sensitized solar cells (DSSCs), organic (OPV), and hybrid cells), but all share the advantages of relatively low manufacturing, transportation, and installation costs, and overall preferable life cycle characteristics compared to conv-PVs that are deposited on thick rigid substrates [12–14]. For greenhouse applications, STPVs could potentially be deployed in larger coverage areas than would otherwise be acceptable with conv-PVs in terms of shading due to their transparency. From an electricity generation standpoint, this design advantage could compensate for relatively lower efficiency of STPVs compared to conv-PVs.

Of the STPV technologies, OPV has a number of material properties that make it uniquely promising technology for integration with greenhouses, including solution processability, spectral tuneability, and mechanical flexibility. Additionally, with regard to production, the solution processability of OPVs means that OPV device fabrication can be implemented with roll-to-roll printing technologies, thus enabling large-scale, continuous production at a fraction of the capital cost and energy input of conv-PV systems, and still lower than other STPV alternatives [15,16]. Environmentally, OPVs are considered preferable even to other STPV technologies, given the fact that OPVs' material components are largely sourced from abundant earth materials and are recyclable/recoverable [13].

The spectral properties of OPVs are important to consider for integration into any transparent or translucent surfaces (e.g., windows, screens, greenhouse covers) in order to determine the effect on transmitted light. A key figure of merit for any STPV technologies is the light utilization efficiency (LUE), equal to the product of the power conversion efficiency (PCE) and the average visible transmission (AVT), which is the weighted transmission spectrum of the STPVs against the photopic response of the human eye [17]. For greenhouse applications, the plant response to light transmitted through the OPV material is of greater consequence than the human eye response. This issue was addressed by Emmott et al. [18] in a modeling study of the techno-economic potential for OPV-integrated greenhouses, in which a crop growth factor (G) was used instead of AVT in an optical model that quantified the effect of various spectrally-selective OPV materials on greenhouse crops. This metric G considered the relative photosynthetic efficiency of the average crop plant at different light wavelengths, based on the work of McCree [19]. Based on this analysis, the authors demonstrated that attaining higher efficiencies and high transparency contact materials were the most important factors in determining OPV suitability for a greenhouse, rather than the absorbance or lack thereof of the OPV material in the photosynthetically active radiation (PAR) range, which includes light wavelengths between 400 to 700 nm.

In hot regions, excessive solar radiation during the summer season requires the application of shading methods (e.g., whitewashing, external shade netting, internal shade screens, transparent spray agents reflecting NIR light, etc.) in combination with the greenhouse ventilation/cooling systems to lower cooling loads and maintain desired growth

conditions for the crop. Depending on the method, solar radiation transmittance can be decreased by 30–50% compared to non-shaded greenhouses [20]. For these locations, greenhouse-integrated OPVs could serve the dual purpose of electricity generation and shading. This potential role for greenhouse-integrated OPVs in high solar insolation regions was addressed by Okada et al. [5], in which lettuce yield and electricity production in an OPV-integrated greenhouse system were simulated in a hot, arid climate (Arizona). It was determined that OPV roof coverage ratios of 50% and 100% during the summer could extend the growing season due to the shading provided, and 49% OPV coverage was sufficient to meet the energy demands of the off-grid greenhouse modeled in the study, with the achievement of the desired lettuce crop yields. Likewise, in an energy-balance modeling analysis of an OPV-integrated greenhouse design conducted by Ravishankar et al. [21], assuming an OPV cell efficiency of approximately 10%, with 85% roof coverage of a glass greenhouse (219 m^2) covered by photoactive OPV area, it was shown that the OPV system was able to produce more than enough electricity to cover the energy requirements of a greenhouse tomato production system in an arid climate such as Arizona. Building on this work, Hollingsworth et al. [22] examined the life-cycle environmental and economic impacts of OPV-integrated greenhouses compared to non-PV-powered and conventional-PV-powered greenhouses and concluded that OPV-integrated greenhouses could outperform the alternatives if there were not significant reductions in crop yields due to OPV-related shading effects.

Evidently, the potential scope of the use of OPVs for greenhouse applications is in large part dependent on understanding the effects of the OPV light modification on the greenhouse microclimate and crop. The response of greenhouse crops to the lighting conditions resulting from the integration of STPV technologies with the greenhouse structure is an increasingly researched topic [23]. A number of these studies have experimented with tomato plants, a major greenhouse vegetable crop worldwide, which is often shaded in high-light regions to mitigate heat stress and fruit quality issues caused by high radiation intensities and air temperatures [24].

Li et al. [25] evaluated resource use efficiency, greenhouse microclimate, and crop yields in a greenhouse covered with glass laminated with luminescent solar concentrator-based PV cells. The PV system evaluated exceeded the energy demands of the 103 m^2 research greenhouse facility located in Tucson, Arizona, equipped with wet-pad and fan cooling system and a natural-gas-based heating system, growing cherry tomatoes with 25.3% more light use efficiency (LUE) in the PV-covered greenhouse compared to the control greenhouse that was covered with double-layer acrylic.

Hassanien et al. [10] investigated the effect of shading by mono-crystalline silicon semi-transparent panels mounted on top of a polycarbonate-covered greenhouse, occupying 20% of the roof area, on the growth of container tomatoes. It was determined that there were no significant differences in the growth of the tomato plants in the PV-integrated greenhouse compared to the unshaded greenhouse.

Ntinas et al. [26] tested a hydroponic tomato cultivation system for medium-sized and cherry varieties in two glass greenhouses, with one greenhouse outfitted with a DSSC cover and the other greenhouse serving as a control. A variety of plant physiological and productivity parameters were measured to determine the effects of the filtered lighting resulting from the integrated DSSC cover. Illuminance was reduced by 20% in the DSSC greenhouse compared to the control. Although the results showed that plants grown in the DSSC greenhouse were found to have relatively lower yields overall, it was found that the shading in the DSSC greenhouse during the summer season was beneficial for the qualitative characteristics of the tomato fruits.

Friman-Peretz et al. [27] compared the microclimate and tomato crop response between a polytunnel with OPVs installed on the roof, contributing 23% shading to the growing space, and a control greenhouse over two seasons in 2018 and 2019 in a Mediterranean climate. Air temperature and humidity levels inside the OPV greenhouse were found not to be significantly different compared to the control. Radiation distribution

inside the OPV greenhouse was less homogenous than the control due to the gaps between the OPV strips deployed on the greenhouse roof. The cumulative yield and average fruit mass were higher in the OPV greenhouse in 2018 and not significantly different in 2019 when a 25% shade cloth was installed on the control greenhouse.

Until now, greenhouse studies evaluating the effects of integrated STPVs, including OPVs, on the tomato crop response and microclimate have experimented with limited/partial shading treatments (less than 25%). As mentioned previously, for greenhouses located in hot and sunny regions, higher shading may be required/desired during the spring and summer production seasons. In order to determine the feasibility of using semi-transparent OPVs as a realistic alternative for conventional greenhouse shading methods, it is critical to test higher shading treatments, which are more representative of typical cultural practices in such regions. Higher shading treatment also involves larger areal coverage by the OPV materials on/in greenhouses—the relatively low efficiency of OPVs compared to silicon PVs necessitates a larger coverage areas, which for this design application would also be desired in order to achieve high shading treatments. The present study addresses the lack of large-scale experimental research into the application of OPVs as a seasonal greenhouse shading method for hot and arid regions. Flexible, semi-transparent, roll-to-roll printed OPV arrays were installed as a roof shade cover on a greenhouse hydroponic tomato production system in a dry, desert region (southern Arizona) characterized by high air temperatures and radiation intensities in the spring and summer. Analyzing the effects of a relatively high OPV shading treatment on the greenhouse microclimate and tomato crop growth and yield, this study provides insights and recommendations for the design and application of greenhouse-integrated OPV shading elements.

2. Materials and Methods

2.1. Study Greenhouse

The study greenhouse was located at the University of Arizona Controlled Environment Agriculture Center in Tucson, Arizona (latitude: 32°16′ N, longitude: 110°56′ W, altitude: 728 m). Figure 1 shows a 3-D schematic of the greenhouse structure, which was developed in a Rhinoceros CAD environment (Robert McNeel & Associates, Seattle, WA, USA) [28]. The greenhouse had a 9.1 m × 14.6 m footprint with 1.8 m sidewalls and a height of 4.9 m at the roof apex, a gothic-arch roof profile, and a true north-south orientation (Golden Pacific Structures, Cincinnati, OH, USA). The greenhouse cover material was double-layer, air-inflated 8-mm low-density polyethylene (LDPE) plastic with a light transmittance of approximately 75% for all solar radiation wavelengths and 65% in the PAR range. The greenhouse climate control system (EnviroStep, Wadsworth, Arvada, CO, USA) controlled air temperature via evaporative cooling with a wet-pad and two exhaust fans positioned on the northern and southern walls, respectively. Two horizontal airflow (HAF) fans located close to the roof in the northwest and southwest quadrants were continuously operating (day and night) to facilitate air distribution throughout the growing space. External environmental conditions were monitored at a climate station positioned at the northern apex of the greenhouse roof, measuring ambient relative humidity and air temperature (HMP60, Vaisala, Helsinki, FI, USA) and horizontal shortwave irradiance with a pyranometer (SP-510, Apogee Instruments, Logan, UT, USA).

2.2. OPV Device Characterization and Installation on Greenhouse Roof

The OPV devices used in this study were PBTZT-stat-BDTT-8 based full solution coated, flexible, semi-transparent organic photovoltaic cells (manufactured by ARMOR Solar Films GmbH, formerly known as OPVIUS GmbH, Kitzingen, Germany). Each 800 mm × 1000 mm OPV panel was comprised of 4 serially-connected OPV modules, with each module containing of ten 12.5-mm-by-660-mm serially-connected cells, with 2.5-mm gaps ('dead area') between the cells; the active area (i.e., areas covered by the cells) constituted 75.8% of each panel. Eight OPV panels were laminated together and wired in parallel to form an OPV array that measured 6400 mm ×1000 mm × 0.6 mm and weighed

approximately 6 kg, with a total active area of 3.4 m^2 per array. The OPV arrays had been deployed in a different design configuration on the greenhouse roof since October 2019 for a previous study characterizing the OPV array electrical performance; 6 OPV arrays were producing power at the time of measurement for the present study.

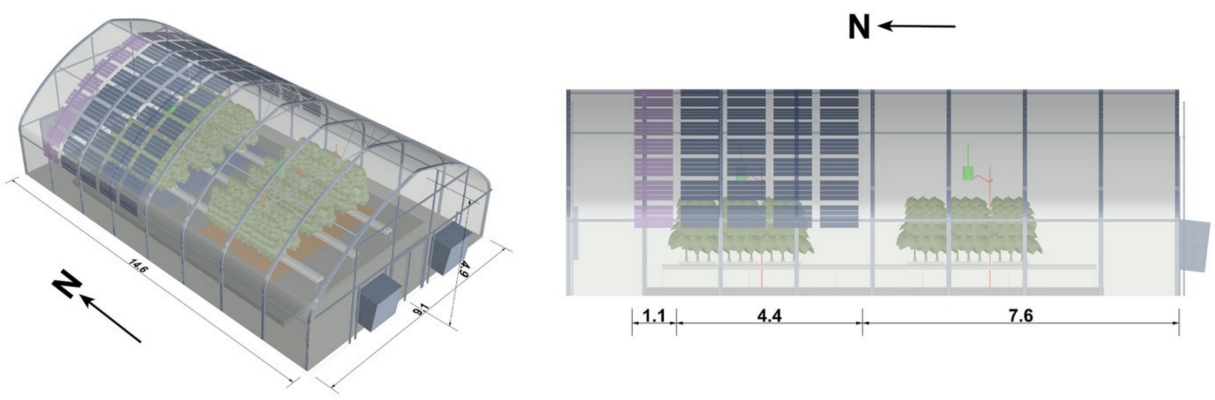

Figure 1. 3-D schematic of the study greenhouse from the southwest view (**left**) with the organic photovoltaics (OPV) shade element installed on the northern section of the greenhouse roof; the view from the west side of the greenhouse (**right**) shows the position of the OPV shade element; two additional OPV arrays (shown in pink) were installed on 11 June 2020. Dimensions are in meters.

The OPV arrays were positioned on the northern section of the greenhouse in a contiguous pattern to fully cover both the east and west greenhouse roof pitches and partially cover the sidewalls (Figure 1). Nylon cord was used to connect the corners of the opposite-facing OPV arrays at the greenhouse roof apex. The opposite end of each array was tied to the greenhouse base near the ground. Additionally, heavy-duty LDPE adhesive tape (GGR Supplies, Miami, FL, USA) was used to adhere the OPV arrays to the polyethylene cover. The OPV shade cover initially comprised eight OPV rolls. Two additional OPV arrays were installed on 11 June 2020 on the northern edge of the OPV shade cover to increase the shaded area, as the solar elevation angle had increased over the course of the study period (see Section 2.2). The total OPV area installed on the greenhouse roof was 51.2 m^2 initially, and then 64 m^2 with the two additional OPV rolls. Thus, the percentage of the OPV shade cover active area was 38.8% initially and then 48.5% with the additional two OPV arrays installed.

Electrical monitoring of the OPV arrays was conducted using an automated current-voltage (I-V) curve measurement system, which was programmed in the Python language. The system operated via serial communication protocol between a laptop (HP, Palo Alto, CA, USA) and a DC programmable electronic load device (8542B, B&K Precision Corporation, Yorba Linda, CA, USA). The OPV arrays were connected to the electronic load, and I-V curves of the OPV arrays were then taken in 10-min intervals during daylight hours (5:00–20:00 h), with the OPV array held at open-circuit between I-V curve measurements. The electronic load device used was capable of monitoring one OPV array at a time, and thus each OPV array was connected to the I-V curve measurement system for a one day of data collection and then subsequently disconnected.

2.3. Shading Effect of the OPV Arrays

Due to the changing solar zenith over the course of the study period, the position of the shading on the greenhouse floor resulting from the OPV shade cover shifted. Figure 2 illustrates the shifting position of the shadows caused by the overhead OPV shade cover on the greenhouse floor during the measurement period; the shadow positions were simulated using the Sun analysis feature in the Rhinoceros CAD program [28], which takes location, date, and time as inputs to calculate the solar angle, and then represents the sun at the calculated angle as a strong directional light cast on the 3-D geometry. The OPV

planting area was positioned such that the central sampling region (see Figure 3) would be continuously shadowed by the OPV coverage for the duration of the measurement period. The northern section of the growing area that was shaded by the OPV is hereafter referred to as the 'OPV section'. The non-OPV shaded section is hereafter referred to as the 'Control section'. The Control section was initially unshaded for 98 days of the study, from 11 March 2020 to 10 June 2020, and then a 30% shade net was installed on the greenhouse roof where the control plants were located on 11 June 2020, enabling a comparison between the OPV shade cover and conventional shading method. The shade net resulted in a relatively proportional decrease in the transmittance of all solar radiation wavelengths in the Control section; its spectral properties are explained further in Section 3.3. The period in which the Control section was unshaded and the period in which the shade net was deployed are distinguished in the reported results.

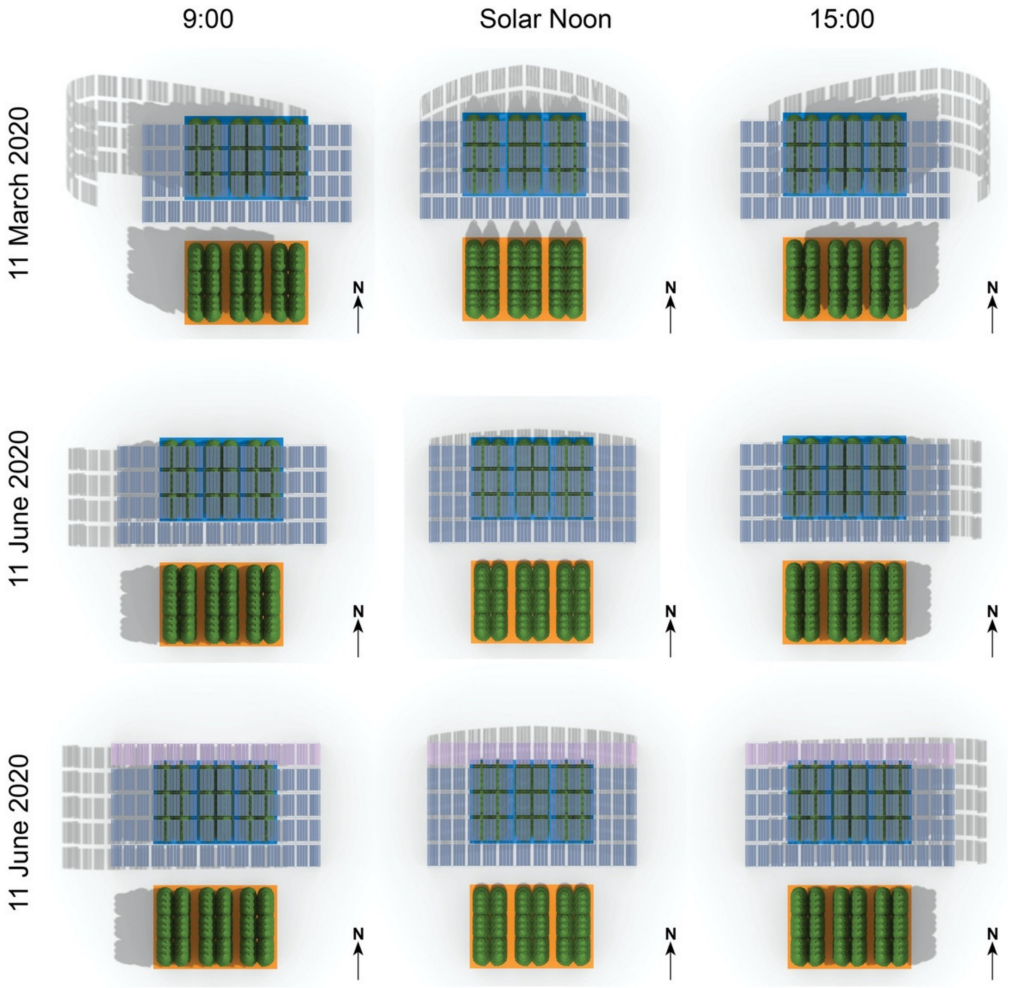

Figure 2. Simulated shadows cast by OPV shade element installed on greenhouse roof on the OPV planting area floor (highlighted in blue), showing the highest amount of southern exposure at the beginning of the measurement period (11 March 2020) and the highest amount of northern exposure (11 June 2020), when two additional OPV arrays were installed to increase coverage.

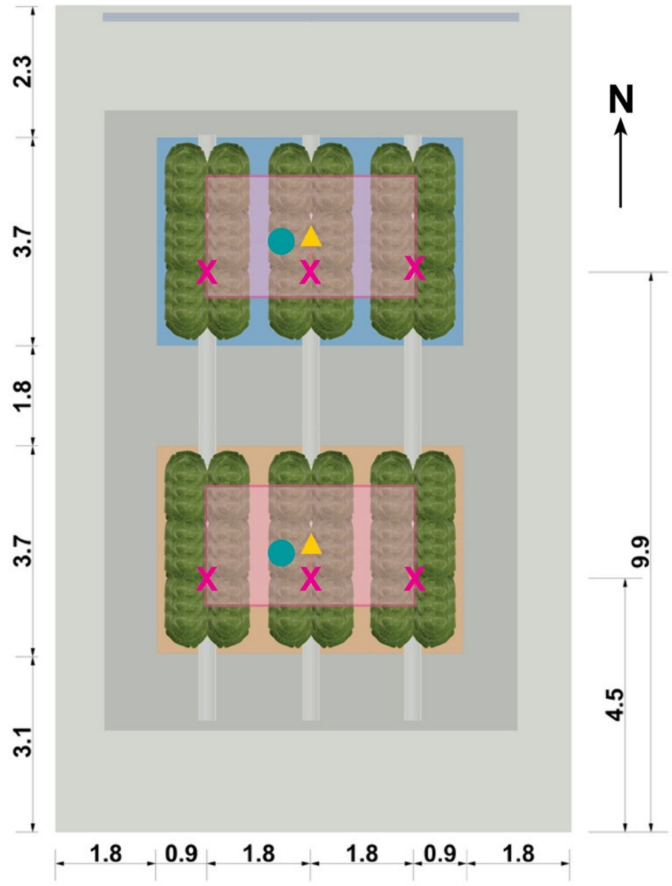

Figure 3. Top view of greenhouse growing area layout, with the OPV and Control planting sections highlighted in blue and orange rectangles (each 17.3 m^2), respectively. The pink rectangles represent the sampling region in each section. The positions of solar radiation sensors (red 'X'), relative humidity/air temperature sensors (blue circle), and infrared radiometers (yellow triangle) are shown. Dimensions are in meters.

2.4. Growing System and Microclimate Monitoring

Figure 3 shows a schematic view of the greenhouse growing area layout and positions of the environmental sensors. One hundred and eight grafted tomato seedlings ('Rebelsky' variety) were transplanted into the growing system on 5 March 2020, and crop data collection began on 11 March 2020. The tomato plants were planted in stonewool cubes fixed to stonewool slabs (GRODAN, Roermond, The Netherlands) in double rows along three gutters with a length of 9.7 m and a gradient of approximately 1%. The distance between the middle of the gutters was 1.8 m. An approximate 1.8-m gap separated the southernmost OPV-shaded plants and the northernmost control plants, with a planting area of 3.7 m × 5.4 m (17.3 m^2) for both the OPV and Control sections (see Figure 2). Each section contained 54 tomato plants, with 9 plants in each of the six rows, resulting in a planting density of 2.70 plants m^{-2} in each section. The growing system was designed and operated as a fully automated recirculating hydroponic system. The OPV and Control sections received the same irrigation schedule and nutrient solution (Hoagland's solution), with EC and pH levels controlled with an automated dosing unit (Intellidose, Autogrow, Auckland, NZ, New Zealand). For the measurement of plant transpiration, lysimeters were positioned to capture irrigation input and drainage from six plants located in the center of each section. The volume, electrical conductivity (EC), and pH of both irrigation input and drainage were measured each morning at around the same time with a handheld EC/pH meter (HI-9814, Hanna Instruments, Smithfield, RI, USA).

All sensor positions in the growing area are shown in Figure 3. Global shortwave

irradiance was measured at the canopy-level using 6 shortwave pyranometers (SP-510, Apogee Instruments, Logan, UT, USA) positioned in the east, center, and west planting areas in both the OPV and Control sections. All solar radiation measurements reported for the OPV and Control sections are averaged values from the east, center, and west pyranometers in the two sections. One air temperature/humidity sensor (HMP60, Vaisala, Helsinki, FI, USA) was located centrally at the canopy-level in each section. Canopy temperature was continuously monitored from 14 May 2020 onward using two infrared radiometer sensors (SI-111-SS, Apogee Instruments, Logan, UT, USA) positioned in the center of the OPV and Control sections (Figure 3).

The measurement period for the crop spanned 126 days (18 weeks), concluding on 11 July 2020. Crop data were collected weekly for 12 randomly tagged sample plants—6 plants per section, located in the inner four rows close to the center of each section (Figure 3). The growth parameters measured both vegetative and reproductive behavior in the crop, specifically head growth (i.e., terminal growth), stem diameter, leaf length, distance of flower growth to the bottom of the apical meristem (i.e., 'tip'), number of fruiting trusses, and the number of open and closed flowers. Yield data were also collected weekly beginning 62 days after transplant (DAT) once fruit had begun to ripen. Yield parameters included total fruit mass, the number of fruits, and average fruit mass. The independent two-sample Student *t*-test with a *p*-value of 0.05 was used to determine statistical significance in the growth and yield parameters measured between the OPV and Control sections.

Lighting quality was measured using a portable spectroradiometer (PS-300, Apogee Instruments, Logan, UT, USA) both outside the greenhouse and in the same positions as the pyranometers on two clear-sky days (20 and 22 May 2020) in the morning, midday, and afternoon, with additional measurements taken of the Control section once the shade net was installed. The spectroradiometer measurements indicate the intensity of shortwave radiation wavelengths between 300–1000 nm incident on the plant canopy in both the OPV and Control sections. Estimates of PAR, typically represented in μmol m^{-2} s^{-1}, incident on the crop canopy in the OPV and Control sections were calculated. These estimates were based on simultaneous measurements taken with a handheld full-spectrum quantum meter (MQ-501, Apogee Instruments, Logan, UT, USA) and a handheld shortwave pyranometer (MP-200, Apogee Instruments, Logan, UT, USA) taken in multiple locations under the OPV shade and under the polyethylene in the Control section. A generalized ratio for PAR to shortwave radiation was determined: in the OPV section, the ratio was 1.81 μmol m^{-2} s^{-1} of PAR for every 1 W m^{-2} of shortwave radiation; in the Control section, the ratio was 2.11 μmol m^{-2} s^{-1} of PAR for every 1 W m^{-2} of shortwave radiation. These ratios were applied to the continuous canopy-level shortwave radiation measurements to estimate canopy-level PAR, which is presented in the analysis as weekly average values. All continuously monitored conditions inside and outside the greenhouse were sampled every 15 s and averaged every 10 min, with average values recorded on two dataloggers (CR-3000 and CR-1000, Campbell Scientific, Logan, UT, USA).

3. Results and Discussion

3.1. Comparison of Microclimate in OPV and Control Sections

Figure 4 shows the average hourly fluctuations in air temperature, relative humidity, and canopy-level shortwave solar radiation in the OPV and Control sections of the study greenhouse for each month of the growing period. The average values for daytime and nighttime periods, along with outdoor conditions, are summarized in Table 1. The average daytime temperature was quite similar in the OPV and Control sections, differing by less than 0.5 °C on average for the duration of the growing period. Given the relatively short distance between the two planting sections and air circulation provided by the ventilation system and HAF fans, this result was expected. With the air temperature being relatively consistent across the OPV and Control sections, the relative differences in crop performance

can be attributed mainly to the deployment of OPV on the greenhouse roof, and other environmental factors related to the OPV shade treatment.

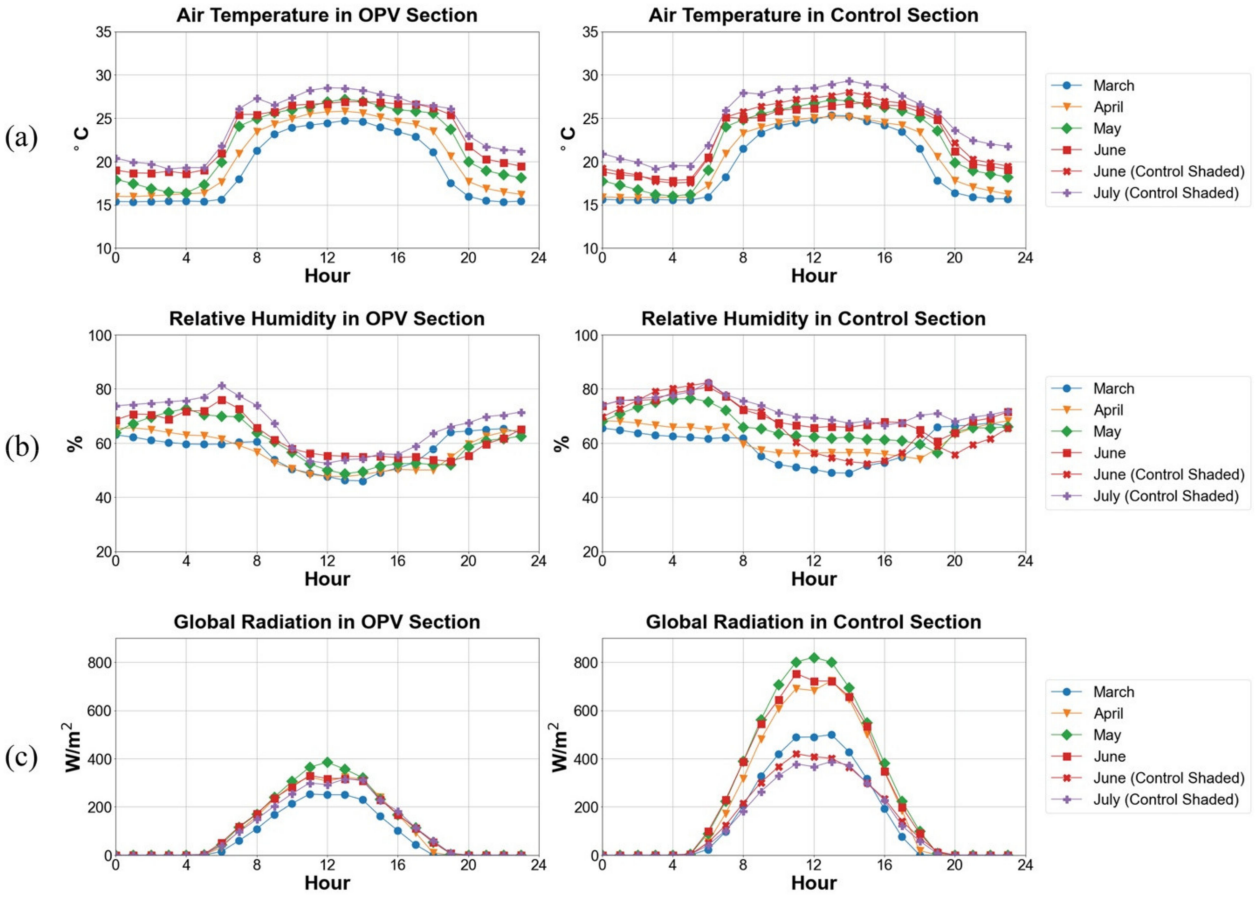

Figure 4. Average hourly values by month for (**a**) air temperature, (**b**) relative humidity, and (**c**) global radiation at the canopy level in the OPV (**left**) and Control (**right**) sections of the greenhouse during the growing period. Global radiation values are averaged from sensors on east, center, and west pyranometers in both OPV and Control sections. A 30% shade net was deployed on the Control section, beginning on 11 June 2020.

The difference in relative humidity (RH) levels between the OPV and Control sections was more pronounced: the OPV section had lower average RH compared to the Control section in both day and night periods for all months, with the magnitude of difference increasing in May and June, corresponding with the highest light-intensity period, until the shade net was installed on the Control section. The daily solar radiation in the OPV section was approximately 35–40% lower than the Control section until the shade net was deployed, at which point the OPV section had 10–15% lower light levels compared to the Control section. It has been established that there is a strong, linearly increasing relationship between greenhouse tomato plant transpiration and solar radiation incident above the crop canopy [29]. The microclimatic differences in relative humidity observed in the OPV and Control sections, which were larger when the Control section was unshaded, can be attributed to the relatively higher transpiration in the Control section canopy, which was also indicated by the direct measurement of transpiration conducted in this study (Table 2), as a result of the relatively higher solar radiation intensities to which it was exposed.

Table 1. Average daytime and nighttime measurements for air temperature, relative humidity, and canopy-level daily solar radiation sum in the OPV-shaded ('OPV') and non-OPV-shaded ('Control') sections of the greenhouse, and outside above the greenhouse. See Materials and Methods section for description of sensor locations.

		Month					
		March	**April**	**May**	**June**	**June**	**July**
Control Section Shade Net (Y/N)		**N**	**N**	**N**	**N**	**Y**	**Y**
Day air temperature (°C)	OPV	22.8	24.0	25.3	25.7	26.2	26.8
	Control	23.2	23.6	25.2	25.3	26.0	27.0
	Outside	19.2	24.6	30.8	32.2	34.9	35.2
Night air temperature (°C)	OPV	15.7	16.7	18.1	19.7	19.5	21.0
	Control	16.0	16.6	18.0	19.3	19.4	21.3
	Outside	12.3	15.0	21.1	24.3	25.1	28.3
Day relative humidity (%)	OPV	52.0	52.0	59.4	64.4	57.6	62.8
	Control	54.1	57.8	65.8	69.4	63.6	71.7
	Outside	38.1	22.4	15.7	17.7	13.4	25.2
Night relative humidity (%)	OPV	62.5	59.4	64.4	65.4	63.2	72.0
	Control	64.8	65.8	69.4	72.1	67.7	73.1
	Outside	64.2	42.1	30.2	28.2	22.5	35.8
Daily solar radiation (MJ/m^2/day)	OPV	6.48	9.32	10.7	9.76	9.86	9.14
	Control	13.6	20.4	22.7	21.4	12.5	11.1
	Outside	18.5	26.7	28.7	28.0	30.3	24.6

Table 2. Average monthly values for daily plant transpiration (mL $plant^{-1}$ day^{-1}) in OPV and Control sections.

		Months				
		April	**May**	**June**	**June**	**July**
Control Section Shade Cloth (Y/N)		**N**	**N**	**N**	**Y**	**Y**
Daily Transpiration (mL $plant^{-1}$ day^{-1})	**OPV**	1587	2264	3316	3101	2381
	Control	1680	2491	4105	3195	2382

Table 2 shows the average monthly values of daily plant transpiration (mL $plant^{-1}$ day^{-1}) during the growing period. For the plants shaded by the OPV cover, the transpiration values were generally lower than the plants in the Control section. The differences in transpiration were higher in May (227 mL $plant^{-1}$ day^{-1} higher in the Control section) and highest in June (789 mL $plant^{-1}$ day^{-1} higher in the Control section); after installation of the shade cover on the Control section, the daily average transpiration of the Control section decreased by 910 mL $plant^{-1}$ day^{-1}, which made the difference between the OPV and Control sections only 94 mL $plant^{-1}$ day^{-1}. In July, the daily average difference in transpiration between the OPV and Control sections was virtually the same. One of the primary functions of shading devices on greenhouses in hot regions is to conserve water, which is spent in crop transpiration as a plant cooling mechanism, as well as in evaporative cooling systems (if used). The unshaded Control plants had 10.2% higher transpiration than the OPV-shaded plants between April and June; once the shade net was installed, the shaded Control plants had 6.9% higher transpiration than the OPV plants in June and July, indicating that water can be saved through greenhouse shading, and in this case, using OPV shade elements.

3.2. Effects of OPV Shading on Canopy Temperature

Figure 5 compares the average hourly canopy temperature of the OPV-shaded plants to that of the Control plants, revealing relatively larger diurnal fluctuations in canopy temperature in the Control section. The OPV shade cover appears to stabilize canopy

temperature during the midday period, with the highest solar radiation intensities, whereas the temperature of the unshaded Control canopy increased during this period.

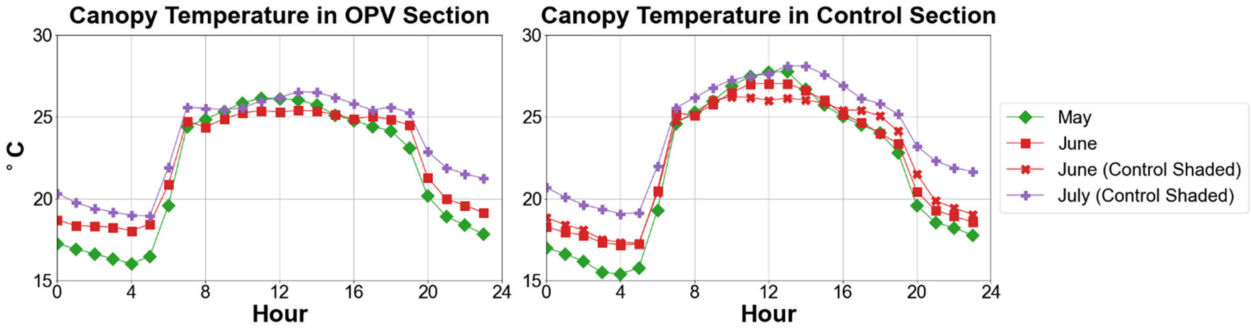

Figure 5. Average hourly values by month for canopy temperature (°C) in the OPV (**left**) and Control (**right**) sections of the greenhouse. A 30% shade net was deployed on the Control section, beginning on 11 June 2020.

Figure 6 presents these results in more detail, showing the canopy temperature, air temperature, and canopy-level solar radiation in the OPV and Control sections of the greenhouse for different environmental conditions in the month of June. For the clear sky day in which no shade net was installed on the Control section (3 June 2020), the canopy temperature in the Control section was 2–3 °C higher than the OPV section during the midday period. Although the air temperature was controlled to relatively consistent levels between the two sections throughout the day, higher solar radiation intensities in the Control section between 10:00–16:00 h increased the canopy temperature over the air temperature level, whereas the OPV-shaded canopy maintained relatively stable temperatures throughout the daylight hours and below the air temperature level. Two days later, when the sky was mostly cloudy, it can be seen that the canopy temperature differences were smaller between the two sections, with sudden increases in canopy temperature coinciding with increased solar radiation levels when the cloud-cover broke. During a clear-sky day later in June when the shade net was deployed over the Control section (23 June 2020), canopy temperatures in that section were more stable throughout the day, although still 1–2 °C higher than the OPV section during the midday period, coinciding with the largest difference in solar irradiance levels between the two sections (approximately 100 W m^{-2}) between 10:00–16:00 h.

Overall, these results, shown in Figure 6, illustrate the effect of solar radiation intensity on plant leaf temperature. Up to a certain point, given sufficient carbon dioxide (CO_2) levels, higher light levels can boost the photosynthetic rate. However, excessive radiation, and especially direct radiation, can also result in overheating of and subsequent tissue damage in the plant, and especially in fruit tissues (which are not as efficient in cooling via transpiration as leaves) [30]. One of the challenges of greenhouse climate control in a desert environment such as southern Arizona is managing the large diurnal outdoor climate fluctuations (e.g., low humidity, high solar radiation intensity, and cooler nights) in order to provide desirable and consistent microclimate conditions for the crop. Shading methods are an integral component of climate control strategies in desert greenhouses during the summer season, assisting ventilation/cooling systems in minimizing microclimate fluctuations [31]. It can be seen in Figure 6 that the OPV coverage served this function as a shade element for greenhouse tomato production during the high-light-intensity period and in the summer season.

3.3. OPV Effects on Lighting Conditions

Figure 7a shows the lighting conditions measured at the canopy-level in both the OPV and Control sections, with and without the shade net deployed on the Control section. The lighting conditions in the Control section had linearly increasing transmittance from the 300–1000 nm range, with relatively lower UV transmittance; the polyethylene film was

coated with anti-UV blocking agents for better stability. The shade net in the Control section caused a relatively constant reduction in the transmittance of all wavelengths measured. For the OPV section, there was a sharp increase in transmittance between 380–440 nm. Between 450–650 nm, there was relatively constant transmittance of around 28%, and then another peak between 660–750 nm.

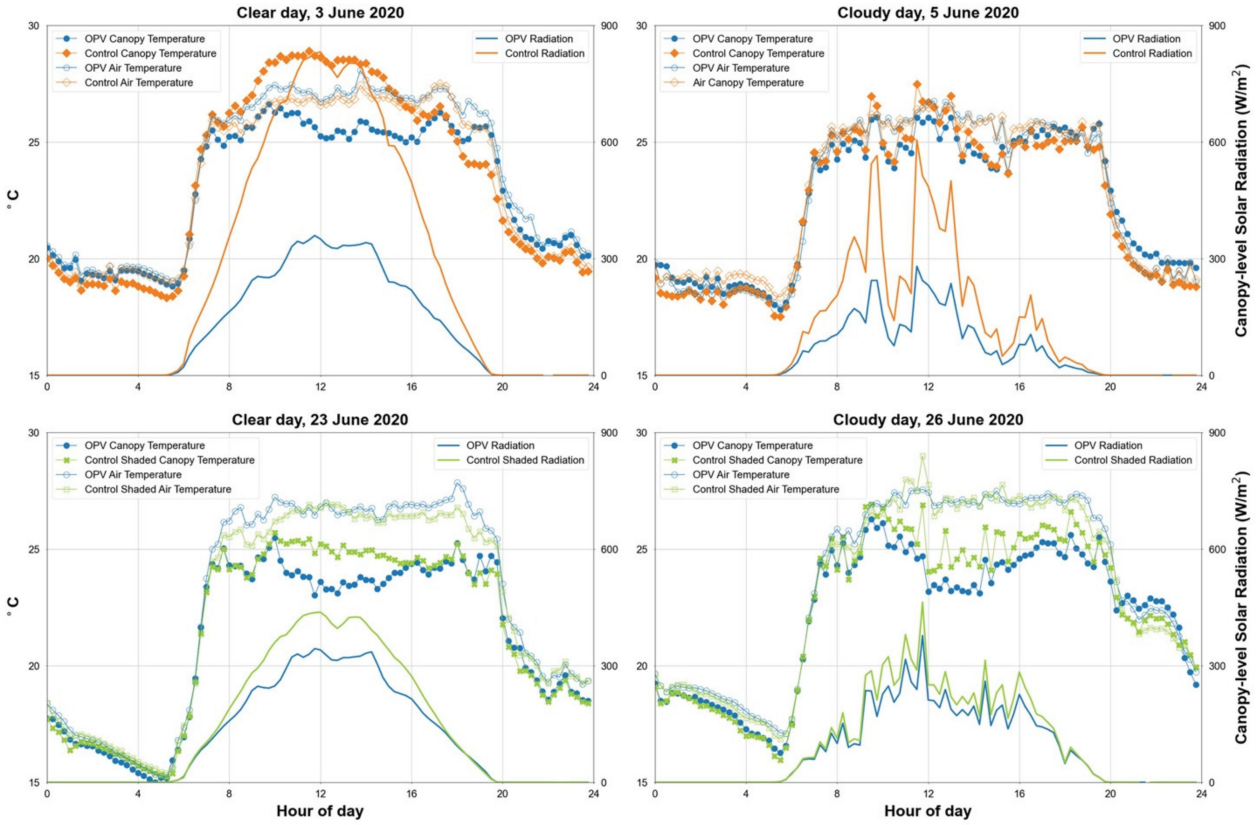

Figure 6. Canopy temperature, air temperature, and canopy-level solar radiation in the OPV and Control sections, comparing conditions in clear (**left**) and cloudy (**right**) sky conditions, and the Control section when it was unshaded (**top**) and when it was shaded by the 30% shade net (**bottom**).

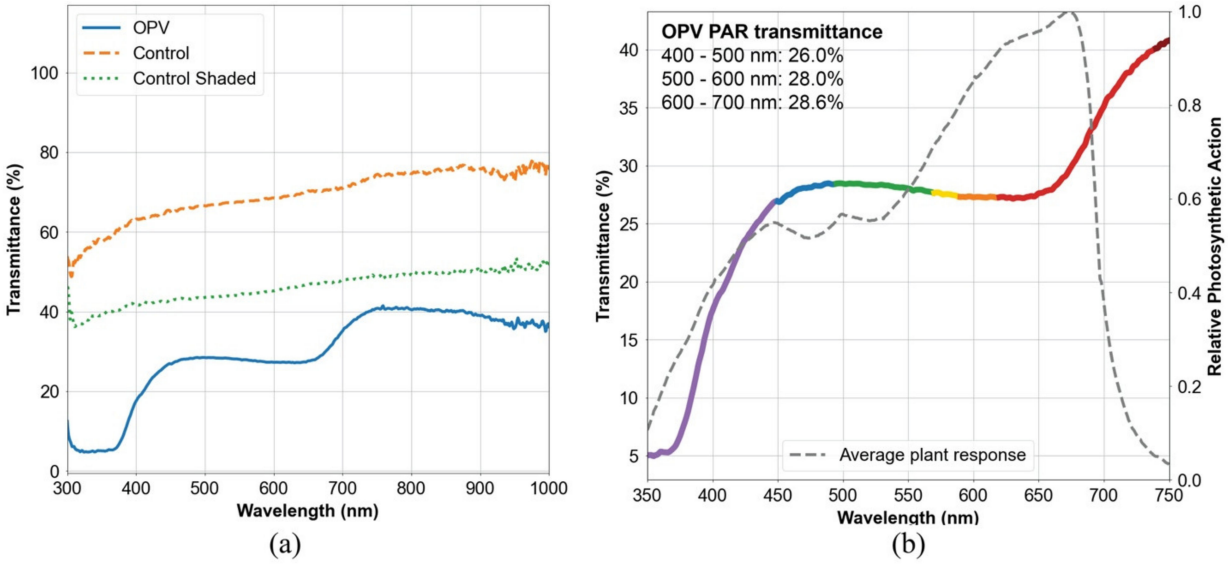

Figure 7. Canopy-level lighting quality in OPV and Control sections: (**a**) comparing OPV and Control sections with and without a shade net installed, measured at midday with a clear sky; (**b**) comparing the light transmittance in the PAR region in the OPV section to the relative photosynthetic action (efficiency), shown in the dashed gray line, which was adapted from McCree [19].

Figure 7b shows the lighting conditions incident on the canopy in the OPV section alongside the averaged relative photosynthetic action of 22 herbaceous crops (i.e., the CO_2 assimilation rate of plants at different ambient light wavelength ranges) [19]. The transmittance of a wavelength-selective semi-transparent OPV shade cover would ideally complement the relative photosynthetic efficiency of the crop in specific wavelength ranges. It can be seen in Figure 7b that the OPV shade cover used in this study was not spectrally optimized for this purpose, although it is worth mentioning that blue photons (between 400–500 nm) are used less efficiently in photosynthesis compared to orange and red photons (600–700 nm) [32]. OPV films that primarily absorb in the near-infrared range (beyond 780 nm) have been developed for greenhouse (and other) applications [33–35], although such technology has not yet been commercialized. However, the goal of spectral optimization should be weighed against other design factors involved in greenhouse-integrated OPV shading strategies. These design factors pertain to the technical features and performance of the OPV (e.g., PCE, transparency, device lifetime), the deployment strategy that is used (e.g., partial vs. full roof coverage), the available solar resources of the target location and in different seasons, and economic considerations (e.g., cost of electricity, cost of OPVs).

For a clear sky, the percentage of solar radiation in the PAR range is approximately 45%; for a fully clouded sky, this percentage increases to approximately 60%, due to the clouds blocking a relatively greater portion of UV and NIR radiation [36]. Although they are mostly transparent, greenhouse cladding materials do not transmit all solar radiation wavelengths equally—although the double-layer polyethylene cover on the greenhouse for this study transmitted ~75% of all solar radiation wavelengths, it can be seen in Figure 7a that the transmittance of PAR radiation was only ~65%; the OPV shade cover decreased transmittance of PAR radiation to the OPV-shaded area to ~28%.

The accumulated daily PAR radiation incident on the crop canopy is known as the daily light integral (DLI) and is measured in $mol_{PAR}\ m^{-2}\ day^{-1}$. Figure 8 presents the estimated weekly averages for the DLI in the OPV and Control sections for the measurement period (see the Materials and Methods section for the calculation procedure). For greenhouse tomato cultivation, the minimum recommended DLI is 15 [37]; a DLI of 30 or above has been suggested as optimal [38], assuming that other environmental conditions (e.g., air temperature, CO_2 availability, root zone conditions) are also maintained at optimal levels. It can be seen in Figure 8 that the DLI values in the OPV section were below the recommended minimum of 15 for 3 weeks, from transplanting until the beginning of April, and then remained above 15 for the duration of the study period. When the Control section was not shaded, the DLI was reduced in the OPV section between 57–65%; the installation of the shade net on the Control section in June narrowed this difference to 31–35%. In terms of targeted DLI levels for tomato cultivation, the OPV shade treatment was excessive when considering the optimal recommended DLI levels.

3.4. Crop Growth and Yield Performance

Figure 9 shows weekly measurements of the vegetative and reproductive growth parameters of the tomato plants located in the OPV and Control sections during the measurement period. The tomato plants grown under the shade of the OPV generally displayed more vegetative growth, specifically, accelerated head growth (i.e., stem elongation) and leaf length on average, and showing a fuller canopy compared to the Control section; this result is attributed to shade avoidance behaviors in the OPV plants, particularly in the initial month after transplant. The differences in head growth and leaf length between the two sections became less pronounced later in the growing season, once the plants had begun the reproductive stage (63 DAT onward). Once the shade net was deployed on the Control section (97 DAT), all growth trends were not found to be significantly different.

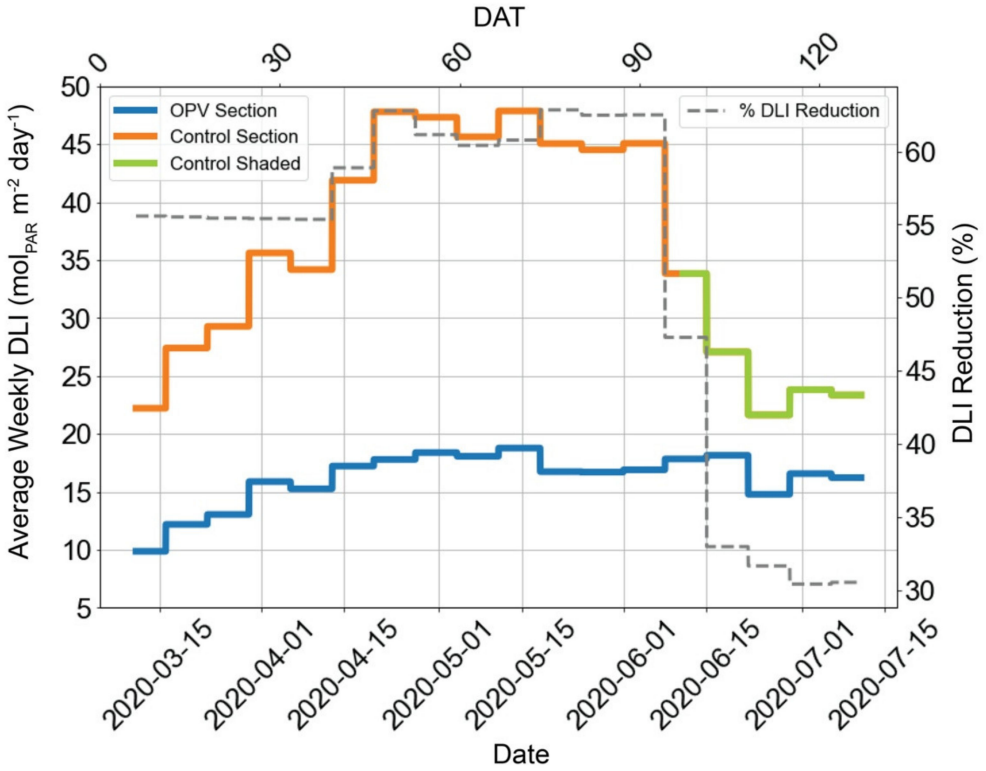

Figure 8. Estimated weekly averages for the daily light integral (DLI, in mol_{PAR} m^{-2} day^{-1}) in OPV and Control sections with corresponding dates and days after transplant (DAT).

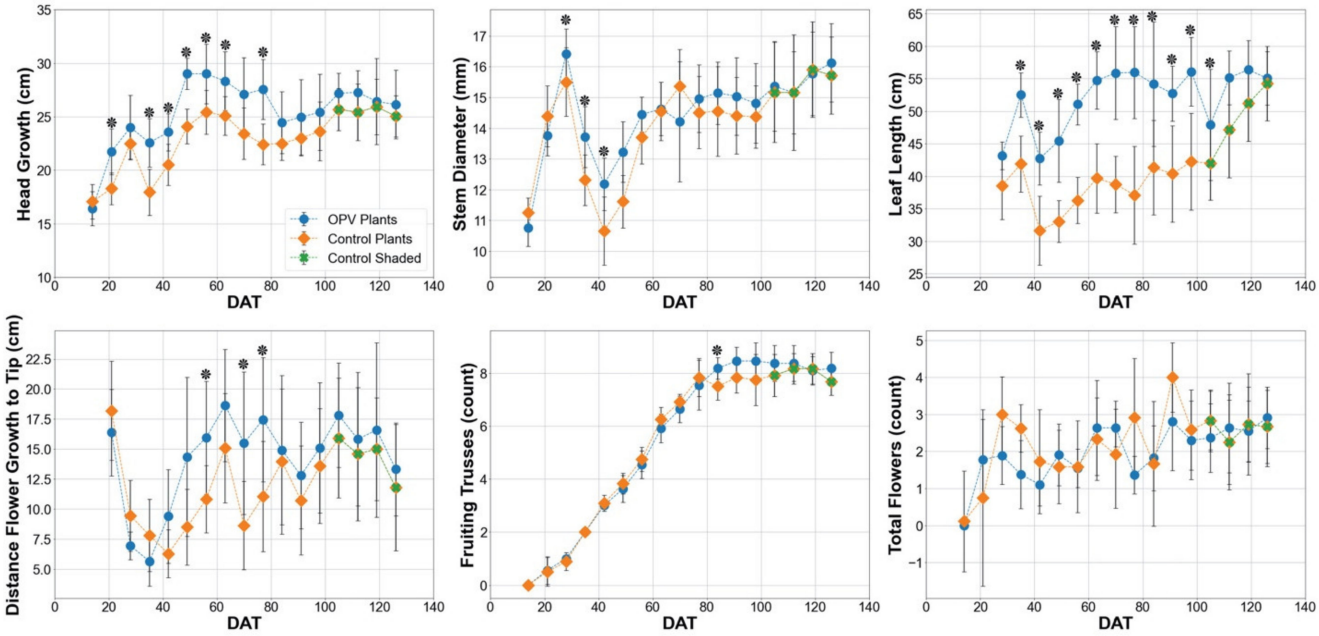

Figure 9. Weekly plant growth in the OPV and Control sections; parameters measured include head growth, head diameter, leaf length, distance of first open flower to plant tip, number of fruiting trusses, and the total number of flowers; days after transplant (DAT); each data point represents the averaged values of 6 sample plants, with bars representing the standard deviation; the ❋ indicates a significant difference based on a two-sample *t*-test statistic, calculated for the OPV and Control sections.

Figure 10 presents the yield productivity in the OPV and Control sections for 10 weekly harvests. The delayed fruit development and ripening in the OPV section is evident in the lower average yields, number of fruits, and average fruit mass compared to the Control section in the first three harvests. Interestingly, the initial three-week period after transplant, in which the DLI levels were estimated to be under the recommended minimum level of 15 (Figure 8), corresponds with the period of lag in the yield productivity of the OPV plants relative to the Control plants. Constrained solar radiation, specifically with reduced DLI, under shade treatments has been shown to limit the growth and development of greenhouse tomatoes [39]. Although the total cumulative yield was somewhat lower in the OPV compared to the Control section (24.6 kg m^{-2} and 27.7 kg m^{-2}, respectively), beginning with the fourth harvest on 83 DAT (28 May 2020), the average yield productivity values in the OPV and Control sections were similar. Between DAT 76–97, reduced yields can be seen in the Control section, whereas the OPV plants showed increased yields, indicating that the OPV plants benefitted from the microclimate conditions created by the OPV cover, mitigating heat stress, which led to yields similar in the control group and even further increases after DAT 80. The deployment of the shade net on the Control section appeared to have a beneficial effect on yield performance in that section.

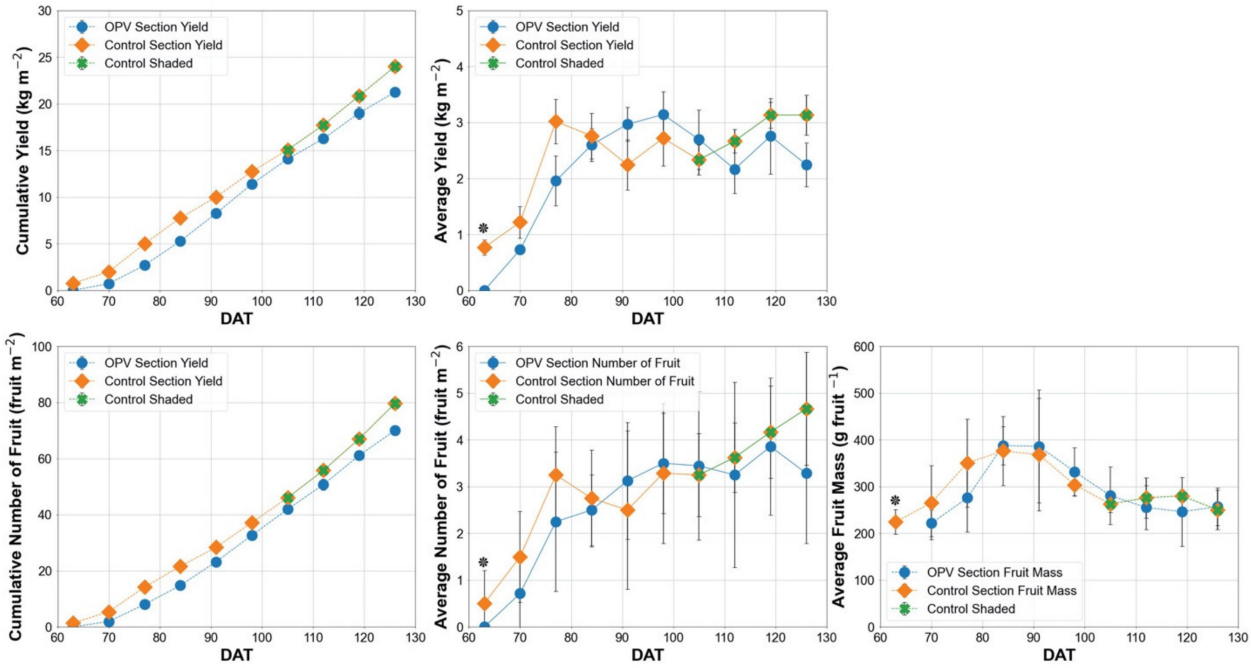

Figure 10. Weekly yield data in OPV and Control Sections for 10 harvests, with the first harvest 62 DAT (7 May 2020) and last harvest 125 DAT (7 July 2020). Each data point represents the averaged value of 6 sample plants located in the inner rows of each section, with bars representing the standard deviation. The ❋ indicates a significant difference between the samples for that week of measurement.

Figure 11 compares the cumulative yield (in kg) in the OPV and Control sections to the cumulative PAR radiation received by the canopy in each section. The linear equations indicate the yield per mole of PAR energy (calculated as g $mol_{PAR}{}^{-1}$) received by the canopy—essentially, the light use efficiency (LUE) of the tomato plants in producing fruit. The LUE in the OPV section was approximately twice as high as that in the Control section, with 21.4 g $mol_{PAR}{}^{-1}$ in the OPV section compared to 10.1 g $mol_{PAR}{}^{-1}$ in the Control section. Once the shade cover was deployed on the Control section, the LUE of the Control section increased to 18.2 g $mol_{PAR}{}^{-1}$, slightly lower than the OPV section. From these results, it can be seen that the plants grown under the OPV shade were able to adapt to the lower light levels reasonably well, with less stress observed under high light intensities, achieving higher weekly yields during the hot and high-light periods, and with

comparable yields to those of the plants grown under a conventional shade net when it was deployed on the Control section. These results clearly indicate the potential of using OPV as a shade element, while also being able to generate electrical energy within the same greenhouse footprint.

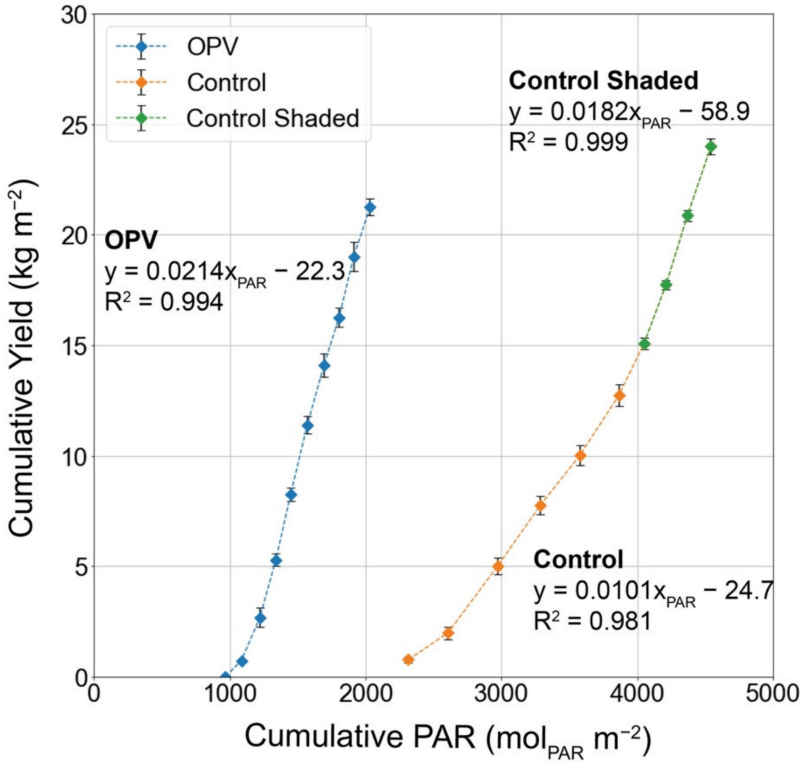

Figure 11. Cumulative yield (in kg m^{-2}) versus cumulative photosynthetically active radiation (PAR, in mol_{PAR} m^{-2}) incident on the canopy in OPV and Control sections. Points represent the averaged values of 6 plants in each section, with bars representing the standard deviation.

3.5. OPV Power Production

Table 3 presents data on the daily power output of six OPV arrays deployed on the east and west pitches of the greenhouse roof. Measurements were taken during a six-day period (23–28 May 2020) with clear skies and an average total daily solar radiation of 8.62 kWh m^{-2} day^{-1}. The electrical performance varied between individual OPV arrays: despite similar solar radiation conditions, the daily power output ranged between 0.056–0.088 kWh m^{-2} day^{-1}. At the time of this measurement, the OPV devices had already experienced a degradation in performance, having been deployed on the greenhouse roof since October 2019 for a previous study that focused on the power generation performance of the OPV arrays. In that study, the average efficiency of the OPV arrays was found to be 1.82%. For the greenhouse (133 m^2 footprint), with the hardware used in this study, the daily energy requirement in the summer season can range between 10–20 kWh day^{-1} (0.075–0.150 kWh m^{-2} day^{-1}) depending primarily on the extent of operation of the wet-pad and fan ventilation/cooling system. Thus, for the daily greenhouse energy requirement to be met during the summer season, an OPV system deployed to fully cover the greenhouse roof would need to achieve 1.1–2.1% efficiencies, which is in the performance range of the OPV devices used in this study. As the OPV industry continues to advance and scale up commercial production, improvement in the quality and stability of large-area OPV products is anticipated. For integrated OPV greenhouse power system design, it should be noted that unless grid-connection is available, batteries or alternative energy storage technologies would need to be included.

Table 3. Power generation performance of six identical OPV arrays deployed on the greenhouse roof, measured on clear-sky days from 23–28 May 2020.

OPV	Location on Greenhouse Roof (East vs. West Pitch)	Date of Measurement	Daily Outdoor Solar Radiation (kWh m^{-2} day^{-1})	OPV Daily Energy Output (kWh m^{-2} day^{-1})
OPV1	East	23 May 2021	8.56	0.056
OPV2	West	25 May 2021	8.56	0.069
OPV4	East	28 May 2021	8.72	0.064
OPV5	West	24 May 2021	8.72	0.080
OPV6	East	27 May 2021	8.64	0.088
OPV7	West	26 May 2021	8.50	0.058

Beyond considerations of OPV performance, however, the design configuration of the OPV arrays used in the present study (i.e., the extensive and symmetrical OPV coverage over the greenhouse roof on both east-facing and west-facing surfaces) resulted in a relatively distributed output of power over the course of the day. This can be seen in Figure 12, which presents the diurnal power generation patterns of the OPV arrays. This installation strategy is advantageous in terms of meeting greenhouse energy requirements throughout the day.

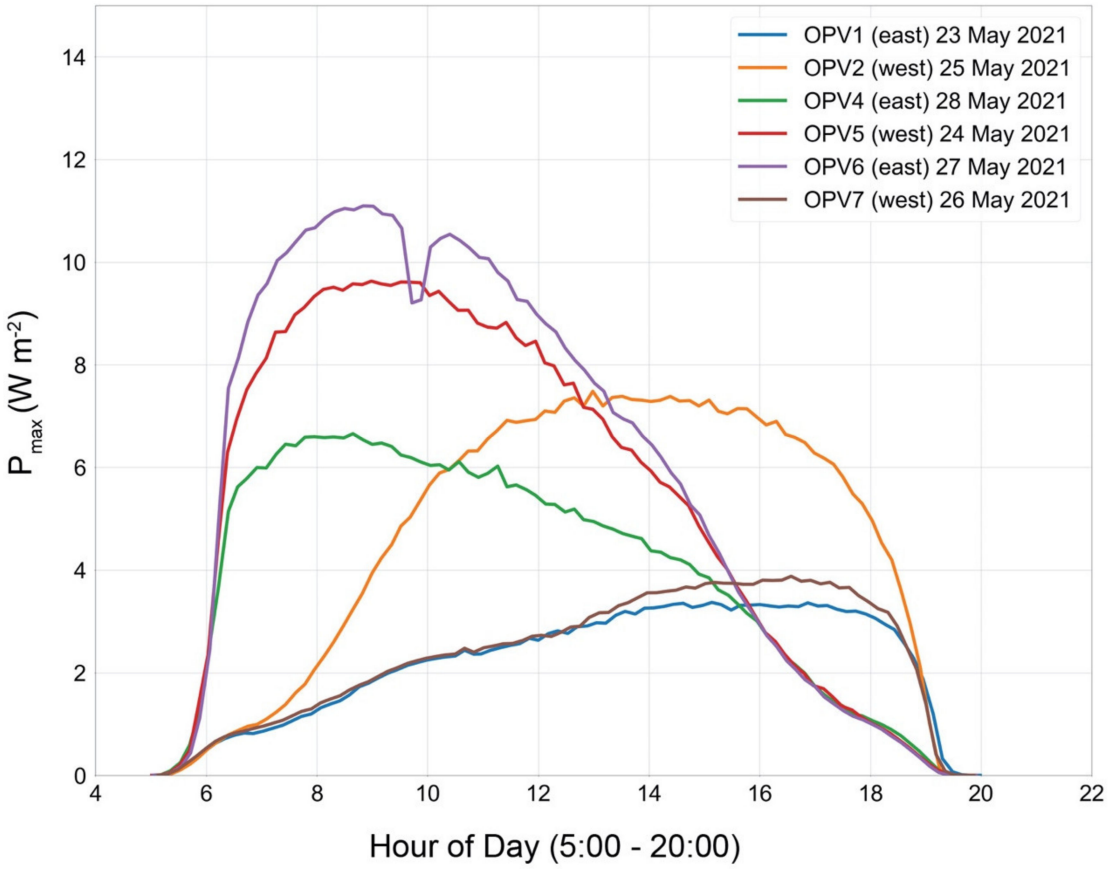

Figure 12. Diurnal power generation patterns (W m^{-2}) of the OPV arrays deployed on the greenhouse roof. The area beneath each curve represents the total daily energy output of each OPV array (in Wh m^{-2}).

4. Conclusions

This study demonstrated the application of commercially manufactured, semi-transparent, flexible, roll-to-roll printed organic photovoltaic (OPV) arrays (3.4 m^2 active area) as a shade element for greenhouse tomato production in a hot, arid climate. The OPV arrays decreased

the transmittance of all solar radiation wavelengths in the shaded area by approximately 40% and photosynthetically active radiation (PAR, 400–700 nm) by approximately 37%.

During the hottest months of the measurement period (May–July), the OPV shade provided a suitable climate for tomato crop production, stabilizing canopy temperature during the times of day with the highest solar radiation intensities, performing the function of a conventional shading method. Constrained solar radiation levels in the OPV section for three weeks following transplant in early March, in which the daily light integral (DLI) values were estimated to be lower than the recommended minimum of 15 mol_{PAR} m^{-2} day^{-1}, resulted in more vegetative growth and delayed fruit development and ripening compared to the Control section, indicating shade avoidance behavior, and leading to lower average yields in the first three (of 10 total) weekly harvests. Beginning with the fourth harvest, however, yield, fruit number, and fruit mass in the OPV and Control sections were similar. Trends in yield productivity for the OPV plants showed increased performance during high-light-intensity periods in May and June. The light utilization efficiency (LUE), which is the relationship between cumulative yield and cumulative PAR radiation, measured in g $mol_{PAR}{}^{-1}$, was approximately twice as high in the OPV section (21.4 g $mol_{PAR}{}^{-1}$) compared to the Control section when it was unshaded (10.1 g $mol_{PAR}{}^{-1}$); during the period in which the Control section was shaded, the LUE increased to 18.2 g $mol_{PAR}{}^{-1}$.

Although the electrical performance of the OPV arrays used for this study varied, the east-west orientation and extensive coverage of the OPVs over the curved greenhouse roof meant that power production could be relatively evenly distributed throughout the day. It can be concluded that the daily electrical energy requirements for the greenhouse in this study with its installed hardware during the summer production season in this region could be met with full roof coverage by OPVs and with efficiencies between 1.1–2.1%, which is in the performance range of the devices used in this study.

Future investigations of OPV applications to greenhouses should test crop types with different light requirements, seasonal effects, effects of OPVs on plant water and nutrient efficiencies, OPVs with different spectral characteristics (higher light transmittance in the PAR spectrum), the effects of degradation on OPVs' spectral characteristics over time, and different OPV installation strategies. The dynamics of energy production/consumption in integrated OPV greenhouse systems should also be explored in future work.

Ultimately, this study demonstrated a readily available design strategy for OPV applications to greenhouses in high-light regions, where shading methods are required for spring and summer greenhouse crop production.

Author Contributions: Conceptualization, R.W., M.K., E.M., M.T., and I.Y.; methodology, R.W.; software, R.W.; validation, R.W.; formal analysis, R.W.; investigation, R.W. and M.K.; resources, M.K.; data curation, R.W.; writing—original draft preparation, R.W.; writing—review and editing, R.W., M.K., E.M., M.T., and I.Y.; visualization, R.W.; supervision, M.K.; project administration, M.K.; funding acquisition, M.K., M.T., and I.Y. All authors have read and agreed to the published version of the manuscript.

Funding: This research was supported by Research Grant No. US-4885-16 from BARD, United States –Israel Binational Agricultural Research and by the National Science Foundation Grant No. DGE1735173 IndigeFEWSS project.

Data Availability Statement: The data presented in this study are available on request from the corresponding author.

Conflicts of Interest: The authors declare that they have no known competing financial interests or personal relationships that could have appeared to influence the work reported in this paper.

References

1. Barbosa, G.; Gadelha, F.; Kublik, N.; Proctor, A.; Reichelm, L.; Weissinger, E.; Wohlleb, G.; Halden, R. Comparison of Land, Water, and Energy Requirements of Lettuce Grown Using Hydroponic vs. Conventional Agricultural Methods. *Int. J. Environ. Res. Public Health* **2015**, *12*, 6879–6891. [CrossRef]
2. Cook, R.L.; Calvin, L. Greenhouse Tomatoes Change the Dynamics of the North American Fresh Tomato Industry. *U.S. Dept. Agric. Econ. Res. Serv.* **2005**, *2*, 1–65.
3. Stanghellini, C.; Montero, J.I. Resource Use Efficiency in Protected Cultivation: Towards the Greenhouse with Zero Emissions. *Horticulturae* **2012**, *927*. [CrossRef]
4. Marrou, H.; Guilioni, L.; Dufour, L.; Dupraz, C.; Wery, J. Microclimate under Agrivoltaic Systems: Is Crop Growth Rate Affected in the Partial Shade of Solar Panels? *Agric. For. Meteorol.* **2013**, *177*, 117–132. [CrossRef]
5. Okada, K.; Kacira, M.; Teitel, M.; Yehia, I. Crop Production and Energy Generation in a Greenhouse Integrated with Semi-Transparent Organic Photovoltaic Film. *Acta Hortic.* **2018**, *1227*, 231–240. [CrossRef]
6. Li, Z.; Yano, A.; Yoshioka, H. Feasibility Study of a Blind-Type Photovoltaic Roof-Shade System Designed for Simultaneous Production of Crops and Electricity in a Greenhouse. *Appl. Energy* **2020**, *279*, 115853. [CrossRef]
7. Marucci, A.; Zambon, I.; Colantoni, A.; Monarca, D. A Combination of Agricultural and Energy Purposes: Evaluation of a Prototype of Photovoltaic Greenhouse Tunnel. *Renew. Sustain. Energy Rev.* **2018**, *82*, 1178–1186. [CrossRef]
8. Marucci, A.; Monarca, D.; Cecchini, M.; Colantoni, A.; Cappuccini, A. Analysis of Internal Shading Degree to a Prototype of Dynamics Photovoltaic Greenhouse through Simulation Software. *J. Agric. Eng.* **2015**, *46*, 144–150. [CrossRef]
9. Bambara, J.; Athienitis, A.K. Energy and Economic Analysis for the Design of Greenhouses with Semi-Transparent Photovoltaic Cladding. *Renew. Energy* **2019**, *131*, 1274–1287. [CrossRef]
10. Hassanien, R.H.E.; Li, M.; Yin, F. The Integration of Semi-Transparent Photovoltaics on Greenhouse Roof for Energy and Plant Production. *Renew. Energy* **2018**, *121*, 377–388. [CrossRef]
11. Lee, T.D.; Ebong, A.U. A Review of Thin Film Solar Cell Technologies and Challenges. *Renew. Sustain. Energy Rev.* **2017**, *70*, 1286–1297. [CrossRef]
12. La Notte, L.; Giordano, L.; Calabrò, E.; Bedini, R.; Colla, G.; Puglisi, G.; Reale, A. Hybrid and Organic Photovoltaics for Greenhouse Applications. *Appl. Energy* **2020**, *278*, 115582. [CrossRef]
13. Muteri, V.; Cellura, M.; Curto, D.; Franzitta, V.; Longo, S.; Mistretta, M.; Parisi, M.L. Review on Life Cycle Assessment of Solar Photovoltaic Panels. *Energies* **2020**, *13*, 252. [CrossRef]
14. Ramanujam, J.; Bishop, D.M.; Todorov, T.K.; Gunawan, O.; Rath, J.; Nekovei, R.; Artegiani, E.; Romeo, A. Flexible CIGS, CdTe and a-Si:H Based Thin Film Solar Cells: A Review. *Prog. Mater. Sci.* **2020**, *110*, 100619. [CrossRef]
15. Riede, M.; Spoltore, D.; Leo, K. Organic Solar Cells—The Path to Commercial Success. *Adv. Energy Mater.* **2021**, *11*, 2002653. [CrossRef]
16. Søndergaard, R.; Hösel, M.; Angmo, D.; Larsen-Olsen, T.T.; Krebs, F.C. Roll-to-Roll Fabrication of Polymer Solar Cells. *Mater. Today* **2012**, *15*, 36–49. [CrossRef]
17. Traverse, C.J.; Pandey, R.; Barr, M.C.; Lunt, R.R. Emergence of Highly Transparent Photovoltaics for Distributed Applications. *Nat. Energy* **2017**, *2*, 849–860. [CrossRef]
18. Emmott, C.J.M.; Röhr, J.A.; Campoy-Quiles, M.; Kirchartz, T.; Urbina, A.; Ekins-Daukes, N.J.; Nelson, J. Organic Photovoltaic Greenhouses: A Unique Application for Semi-Transparent PV? *Energy Environ. Sci.* **2015**, *8*, 1317–1328. [CrossRef]
19. McCree, K.J. The Action Spectrum, Absorptance and Quantum Yield of Photosynthesis in Crop Plants. *Agric. Meteorol.* **1971**, *9*, 191–216. [CrossRef]
20. Ahemd, H.A.; Al-Faraj, A.A.; Abdel-Ghany, A.M. Shading Greenhouses to Improve the Microclimate, Energy and Water Saving in Hot Regions: A Review. *Sci. Hortic.* **2016**, *201*, 36–45. [CrossRef]
21. Ravishankar, E.; Booth, R.E.; Saravitz, C.; Sederoff, H.; Ade, H.W.; O'Connor, B.T. Achieving Net Zero Energy Greenhouses by Integrating Semitransparent Organic Solar Cells. *Joule* **2020**, *4*, 490–506. [CrossRef]
22. Hollingsworth, J.A.; Ravishankar, E.; O'Connor, B.; Johnson, J.X.; DeCarolis, J.F. Environmental and Economic Impacts of Solar-Powered Integrated Greenhouses. *J. Ind. Ecol.* **2020**, *24*, 234–247. [CrossRef]
23. Aroca-Delgado, R.; Pérez-Alonso, J.; Callejón-Ferre, Á.J.; Velázquez-Martí, B. Compatibility between Crops and Solar Panels: An Overview from Shading Systems. *Sustainability* **2018**, *10*, 743. [CrossRef]
24. Peet, M.M.; Welles, G. Greenhouse tomato production. In *Tomatoes*; Heuvelink, E., Ed.; CAB International: Wallingford, UK, 2005; pp. 257–304.
25. Li, W. Resource Use Efficiency under Photovoltaic Integrated Greenhouse Glazing. Master's Thesis, Department of Biosystems Engineering, The University of Arizona, Tucson, AZ, USA, 2014.
26. Ntinas, G.K.; Kadoglidou, K.; Tsivelika, N.; Krommydas, K.; Kalivas, A.; Ralli, P.; Irakli, M. Performance and Hydroponic Tomato Crop Quality Characteristics in a Novel Greenhouse Using Dye-Sensitized Solar Cell Technology for Covering Material. *Horticulturae* **2019**, *5*, 42. [CrossRef]
27. Friman-Peretz, M.; Ozer, S.; Geoola, F.; Magadley, E.; Yehia, I.; Levi, A.; Brikman, R.; Gantz, S.; Levy, A.; Kacira, M.; et al. Microclimate and Crop Performance in a Tunnel Greenhouse Shaded by Organic Photovoltaic Modules—Comparison with Conventional Shaded and Unshaded Tunnels. *Biosyst. Eng.* **2020**, *197*, 12–31. [CrossRef]

28. *Rhinoceros 3D v7*; Robert McNeel & Associates: Seattle, WA, USA, 2020; Available online: https://www.rhino3d.com/ (accessed on 3 June 2021).
29. Jolliet, O.; Bailey, B.J. The Effect of Climate on Tomato Transpiration in Greenhouses: Measurements and Models Comparison. *Agric. For. Meteorol.* **1992**, *58*, 43–62. [CrossRef]
30. Masabni, J.; Sun, Y.; Niu, G.; del Valle, P. Shade Effect on Growth and Productivity of Tomato and Chili Pepper. *HortTechnology* **2016**, *26*, 344–350. [CrossRef]
31. Giacomelli, G.A.; Kubota, C.; Jensen, M. Design Considerations and Operational Management of Greenhouse for Tomato Production in Semi-Arid Region. *Int. Soc. Hortic. Sci.* **2005**, *691*, 525–532. [CrossRef]
32. Bugbee, B. Toward an Optimal Spectral Quality for Plant Growth and Development: The Importance of Radiation Capture. *Acta Hortic.* **2016**, *1134*, 1–12. [CrossRef]
33. Liu, Y.; Cheng, P.; Li, T.; Wang, R.; Li, Y.; Chang, S.Y.; Zhu, Y.; Cheng, H.W.; Wei, K.H.; Zhan, X.; et al. Unraveling Sunlight by Transparent Organic Semiconductors toward Photovoltaic and Photosynthesis. *ACS Nano* **2019**, *13*, 1071–1077. [CrossRef] [PubMed]
34. Shi, H.; Xia, R.; Zhang, G.; Yip, H.-L.; Cao, Y. Spectral Engineering of Semitransparent Polymer Solar Cells for Greenhouse Applications. *Adv. Energy Mater.* **2019**, *9*, 1803438. [CrossRef]
35. Song, W.; Fanady, B.; Peng, R.; Hong, L.; Wu, L.; Zhang, W.; Yan, T.; Wu, T.; Chen, S.; Ge, Z. Foldable Semitransparent Organic Solar Cells for Photovoltaic and Photosynthesis. *Adv. Energy Mater.* **2020**, *10*, 2000136. [CrossRef]
36. Meek, D.W.; Hatfield, J.L.; Howell, T.A.; Idso, S.B.; Reginato, R.J. A Generalized Relationship between Photosynthetically Active Radiation and Solar Radiation. *Agron. J.* **1984**, *76*, 939–945. [CrossRef]
37. Runkle, E. *DLI "Requirements" Technically Speaking*; Greenhouse Product News Magazine: Sparta, MI, USA, 2019.
38. Dorais, M. The Use of Supplemental Lighting for Vegetable Crop Production: Light Intensity, Crop Response, Nutrition, Crop Management, and Cultural Practices. In Proceedings of the Canadian Greenhouse Conference, Niagara Falls, ON, Canada, 9 October 2003.
39. Kläring, H.P.; Krumbein, A. The Effect of Constraining the Intensity of Solar Radiation on the Photosynthesis, Growth, Yield and Product Quality of Tomato. *J. Agron. Crop Sci.* **2013**, *199*, 351–359. [CrossRef]